

Search for $n-\bar{n}$ Oscillation in Oxygen

T. W. Jones, R. M. Bionta, G. Blewitt, C. B. Bratton, B. G. Cortez,^(a) S. Errede, G. W. Foster,^(a) W. Gajewski, K. S. Ganezer, M. Goldhaber, T. J. Haines, D. Kielczewska,^(b) W. R. Kropp, J. G. Learned, E. Lehmann, J. M. LoSecco, H. S. Park, F. Reines, J. Schultz, E. Shumard, D. Sinclair, H. W. Sobel, J. L. Stone, L. R. Sulak, R. Svoboda, J. C. van der Velde, and C. Wuest

(Irvine-Michigan-Brookhaven Collaboration)

The University of California at Irvine, Irvine, California 92717, and The University of Michigan, Ann Arbor, Michigan 48109, and Brookhaven National Laboratory, Upton, New York 11973, and California Institute of Technology, Pasadena, California 91125, and Cleveland State University, Cleveland, Ohio 44115, and The University of Hawaii, Honolulu, Hawaii 96822, and University College, London WC1E 6BT, United Kingdom

(Received 24 October 1983)

This Letter reports the results of a search for neutron-antineutron transitions in oxygen, using a water Cherenkov detector of fiducial mass 3300 metric tons located 1570 m (water equivalent) underground. Two independent methods yield 90% confidence lower limits of 1.7×10^{31} and 2.4×10^{31} yr, respectively, for the partial lifetime of this process. According to recent calculations the latter result corresponds to a lower limit in the range 2.7×10^7 to 1.1×10^8 sec for the free-neutron oscillation time.

PACS numbers: 14.20.Dh, 23.90.+w

Recent theories unifying the basic forces of nature admit the possibility of both nucleon decay ($\Delta B=1$) and neutron-antineutron transition ($\Delta B=2$) processes. To take two examples, the standard SU(5) model¹ predicts nucleon decay and forbids n to \bar{n} transitions, whereas the partial unification scheme of Mohapatra and Marshak² forbids nucleon decay and allows $n\bar{n}$ transitions, albeit at an uncertain rate. The phenomenology of $n\bar{n}$ oscillations in nuclei has recently been reviewed by Mohapatra.³

The Irvine-Michigan-Brookhaven (IBM) detector has been briefly described in previous Letters.⁴ For the purposes of this report it is sufficient to recall that the detector consists of a large rectangular volume of purified water ($17 \times 18 \times 23$ m³) viewed from its six faces by 2048 photomultiplier tubes (PMT), each of 12.5 cm diameter, located on a rectangular grid of ~ 1 m spacing. The mass of the detector inside the PMT planes is 7000 metric tons (tonnes) and the fiducial volume in which $n\bar{n}$ transitions are searched for is inset by 2 m from these planes and contains 3300 tonnes of water.

Relativistic charged particles traversing the detector produce Cherenkov photons which fire the photomultiplier tubes. The arrival time (T_1) and the pulse height (Q) for each hit tube are recorded. This information allows the reconstruction of position, direction, and energy of particles moving in the detector. Furthermore, the decay electron from the $\pi^+ \rightarrow \mu^+ \rightarrow e^+$ decay chain,

or more rarely from π^+ decay in flight, where the μ^+ comes to rest, can be detected on a separate slow time scale (T_2). The detection efficiency for such muon decays is 62%, obtained by requiring five or more lit tubes in a 60-ns coincidence window on the slow time scale. The contamination caused by accidentals in this case is about 1.5% per event. These numbers are determined from a sample of cosmic-ray muons and are consistent with a Monte Carlo simulation.

Since $n\bar{n}$ and $p\bar{n}$ annihilation events in oxygen are expected to have several pions in the final state, two methods have been used to detect such events in the IBM detector. The first looks simply for two or more decay electrons in the T_2 scale from multiple π^+ decays and requires the event to consist of more than one track identified in the T_1 scale by a scanning by a physicist. The second method looks for events which produce significant isotropic light, as discussed later in more detail. Both methods required that the number of prompt (T_1) hits be greater than fifty. Events can be simulated in the detector with Monte Carlo techniques which have been calibrated by use of the known properties of through-going and stopping muons.

In order to estimate the detection efficiency of these methods, which will be described in detail in a future paper, two calculations are required:

Firstly, $n\bar{n}$ and $p\bar{n}$ annihilations must be generated in the oxygen nucleus. Use was not made of \bar{p} or \bar{n} annihilation data in nuclei since the pub-

lished data are meager, annihilation occurs at the nuclear periphery, and the \bar{n} data⁵ are for \bar{n} annihilation at 600 MeV rather than at rest. Instead, $\bar{p}p$ and $\bar{p}d$ data⁶⁻⁸ from hydrogen and deuterium bubble chambers were used to determine the branching ratios for the various multipion modes. The kinematics were determined by relativistic phase-space distributions with some modifications for ω production at the 13% level. Since the ω meson is comparatively long lived and 71% of them emerge from the nucleus, its decay products can escape nuclear reinteraction effects. (Pions around 200 MeV strongly excite the first Δ resonance at 1232 MeV with a mean nucleon cross section as high as 135 mb.) The calculated charged-pion momentum spectrum and the charged- and neutral-pion multiplicities are in good agreement with the data of Horwitz *et al.*⁹

Annihilation events within the nucleus were generated according to the comparatively peripheral distribution predicted by Dover, Gal, and Richard.¹⁰

Secondly, pions from the annihilation must be propagated through the nucleus and through the water of the detector. A detailed understanding of the pion-nucleus interactions in the Δ region does not exist.¹¹ Indeed, reasonably detailed and complete measurements of the elastic (σ_{el}), inelastic (σ_{inel}), charge-exchange (σ_{chx}), and absorption (σ_{abs} —where no pion emerges) cross sections in nuclei have become available only recently.¹²

It is accepted that the Δ resonance dominates, such that inelastic scattering proceeds by the pion interacting with a bound nucleon to make a Δ resonance. The resonance then propagates through nuclear matter. Provided that the Δ is not absorbed, the final result will be inelastic or charge-exchange scattering depending on the decay mode of the Δ . The cross section for these processes can be reasonably related to the corresponding elastic and charge-exchange cross sections off free protons, provided that the effects of Fermi motion and Pauli blocking are taken into account. If the Δ interacts with another nucleon in the nucleus to produce two nucleons, then no pion is emitted. If we assume that a dinucleon process is involved, it is reasonable to assume that the absorption probability in the nucleus is proportional to the square of the local

nucleon density. Since single-nucleon processes depend linearly on this density, inelastic scattering dominates in the nuclear periphery, and absorption in the central region of the nucleus.

The above assumptions have been taken as reasonable starting hypotheses in a pion cascade model in which the oxygen matter density is taken from electron-scattering data.¹³ Its predictions for the scattering of an incoming pion are then compared with pion-oxygen data interpolated from the pion-nucleus cross sections reported by Ashery¹² for a range of nuclei from lithium to bismuth. As a first approximation, the absorption probability is taken to be $C\sigma_{\pi d}\rho^2$, where C is an adjustable parameter, $\sigma_{\pi d}$ is the πd cross section, and ρ is the local nuclear matter density. Since the use of π^+d cross section is at best a first guess, its energy dependence is then distorted so as to improve the agreement the model predictions and the data.

Figure 1 shows that the model can be adjusted to agree reasonably well with the data. The model is also run in the $n\bar{n}$ mode with the same assumptions used in analyzing the pion-scattering mode. The same oxygen data and pion-nucleon data allow the prediction of the fate of charged pions in the water.

The expected mean number of tube hits $N(T_1)$, and their standard deviations (S.D.), obtained from the simulation of $n\bar{n}$ events in water are summarized below:

	$N(T_1) \pm S.D.$
No nuclear or N ₂ O effects	200 \pm 47
H ₂ O effects only	185 \pm 55
Nuclear and H ₂ O effects	150 \pm 55

With nuclear and H₂O effects included 25% and 7% of the events will have two- and three-muon decays, respectively. This stopping rate leads to the overall efficiency of 14% for event signatures with two or more decays. (If the distribution of annihilation events follows the matter distribution in the nucleus and ω production is also neglected, the efficiency would be reduced to 11%.) The annihilation events pass through the complete analysis chain with an efficiency of 85%.

Since none of the 109 contained events found in the 132 d of live time has two-decay signatures and at the same time satisfies the number-of-tubes and multitrack requirements, this method gives the following lower lifetime limit:

$$\tau(n \rightarrow \bar{n}) > \frac{(8.9 \times 10^{32} \text{ neutrons})(0.36 \text{ yr})(0.14 \times 0.85 \text{ efficiency})}{2.3 \text{ events (90\%-C.L. upper limit)}} = 1.7 \times 10^{31} \text{ yr.}$$

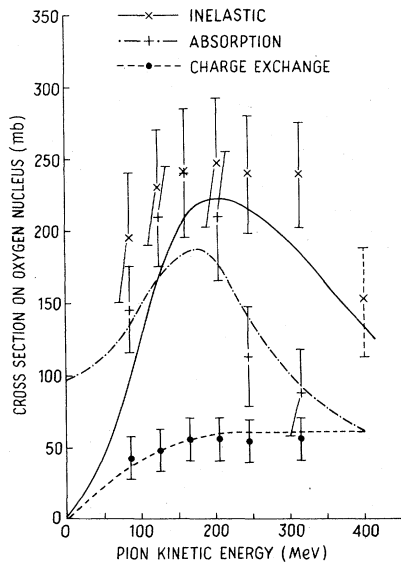


FIG. 1. Comparison of interpolated data for pion-oxygen cross sections with predictions of the nuclear model. The "datum point" at 400 MeV is obtained from the interpolated value of the reaction cross section and with subtraction of 120 mb for $\sigma_{abs} + \sigma_{chx}$.

The second method of searching for $n\bar{n}$ oscillation in oxygen relies on the significant amounts of Cherenkov light emitted isotropically by multi-body annihilations, followed by the reinteraction effects in the nucleus and water described above. A variable, "isotropy angle," is defined which distinguishes these events from the neutrino background events which predominantly produce light in only one hemisphere.

Neutrino, nucleon decay, and $n\bar{n}$ events originating in the fiducial volume are approximately point sources of Cherenkov light in the detector. For multitrack events with significant light in more than a hemisphere the position and timing of the lit tubes are sufficient to locate the vertex to ~ 70 cm. Single-track events require the additional constraint of the Cherenkov angle to achieve a comparable precision.

The recorded PMT hits are extrapolated to a sphere centered on this vertex, and an axis is found about which these hits would have the least moment of inertia, were they mass points. The hits are weighted by photoelectron count (Q) and inversely by absorption in the water. This axis is a good approximation to the true event axis for both single-track and back-to-back events.

A second axis is then found which points along the average direction of all the PMT hits, again weighted for the photoelectron and water absorption, as seen from the vertex. For single-track

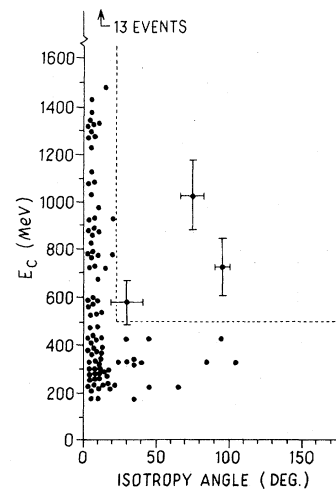


FIG. 2. Cherenkov energy vs isotropy angle for 109 contained events. The horizontal error bars which are typical indicate the uncertainty in angle due to the uncertainty in the vertex position. Vertical error bars represent our $\pm 15\%$ (systematic plus statistical) uncertainty in energy. The dotted lines indicate the region of acceptance for $n\bar{n}$ events.

events this second axis is highly correlated to the first axis whereas for wide-angle multitrack events the two axes are uncorrelated. The isotropy angle is defined as the angle between the first and second axes.

In Fig. 2 the event energy is plotted versus isotropy angle for the 109 data events. (The event energy E_c represents a lower limit on the energy released in the interaction, based on the assumption that all particles are showering and massless. The true energy of the event requires the addition of ~ 250 MeV for each charged pion or muon in the event.) If the isotropy angle and event energy are required to be greater than 20° and 500 MeV, respectively, then 50% of the simulated $n\bar{n}$ events are accepted and pass through the analysis chain. Three data events fall within these cuts. Monte Carlo simulations of the expected background from atmospheric neutrino interactions are consistent with the data in Fig. 1. However, until this background is understood in more detail no background subtraction is made from the three events. Thus, with 6.7 events (90%-C.L. upper limit) and a detection efficiency of 50% the lifetime limit is 2.4×10^{31} yr.

This result is consistent with the above limit of 1.7×10^{31} yr based on the same data sample, and so it is used as the best estimate of the limit.

The calculations of Dover, Gal, and Richard¹⁰ show that in oxygen a bound lifetime $> 10^{31}$ yr

leads to a limit of $\tau_{n\bar{n}} > 5.7 \times 10^7$ sec on the free-space oscillation time. With this result, the bound-lifetime limit of 2.4×10^{31} yr translates to a lower limit on the free-neutron oscillation time of 8.8×10^7 sec.

These calculations are dependent on current knowledge of the antineutron potential in oxygen. Very recently Wong *et al.*¹⁴ found that three potentials are consistent with the \bar{p} -nucleus data in oxygen. The corresponding lower limits on $\tau_{n\bar{n}}$ range from 2.7×10^7 to 1.06×10^8 sec. Also the connection between the bound lifetime and the free oscillation time could be affected by any change in the $n\text{-}\bar{n}$ transition amplitude caused by the nuclear environment, as pointed out by Kabir.¹⁵ Further, Basecq and Wolfenstein¹⁶ suggest that dinucleon to pion transitions can occur in nuclei.

These results should be compared with the preliminary result of $\tau_{n\bar{n}} > 1.0 \times 10^6$ sec for the free $n\bar{n}$ transition at the Grenoble reactor,¹⁷ and the result of Cherry *et al.*¹⁸ of $\tau_{n\bar{n}} > 1.4 \times 10^{30}$ yr for neutrons bound in oxygen.

We wish to thank the many people who helped to bring the IMB detector into successful operation, especially the employees of Morton-Thiokol, Inc., who operate the Fairport mine. The comparatively peripheral distribution predicted by Dover, Gal, and Richard¹⁰ was pointed out to us by G. T. Condo.

^(a)Also at Harvard University, Cambridge, Mass.

02138.

^(b)Permanent address: Warsaw University, 00681 Warsaw, Poland.

¹H. Georgi and S. L. Glashow, *Phys. Rev. Lett.* **32**, 438 (1979).

²R. N. Mohapatra and R. E. Marshak, *Phys. Rev. Lett.* **44**, 1316 (1980), and *Phys. Lett.* **94B**, 183 (1980).

³R. N. Mohapatra, in *Proceedings of the Informal Workshop on Neutron-Antineutron Oscillations*, edited by M. S. Goodman, M. Machacek, and P. D. Miller (Harvard Univ. Press, Cambridge, Mass., 1982).

⁴R. M. Bionta *et al.*, *Phys. Rev. Lett.* **51**, 27 (1983); S. Errede *et al.*, *Phys. Rev. Lett.* **51**, 245 (1983).

⁵H. F. Besch *et al.*, *Z. Phys. A* **292**, 197 (1979).

⁶R. Armenteros and B. French, in *High Energy Physics*, edited by E. H. S. Burhop (Academic, New York, 1969), Vol. 4, p. 237.

⁷P. Pavlopoulos *et al.*, in *Nucleon-Nucleon Interactions—1977*, edited by H. Fearing, D. Measday, and A. Strathdee, AIP Conference Proceedings No. 41 (American Institute of Physics, New York, 1978), p. 340. See in particular the table on page 347.

⁸A. Backenstoss *et al.*, CERN Report No. CERN-EP/83-58, 1983 (unpublished).

⁹N. Horwitz *et al.*, *Phys. Rev.* **115**, 472 (1959).

¹⁰C. B. Dover, A. Gal, and F. M. Richard, *Phys. Rev. D* **27**, 1090 (1983).

¹¹C. H. Q. Ingram, *Nucl. Phys.* **A374**, 319c (1982).

¹²D. Ashery, *Nucl. Phys.* **A354**, 555 (1981).

¹³R. Hofstadter, *Rev. Mod. Phys.* **28**, 214 (1956).

¹⁴C. Y. Wong *et al.*, to be published.

¹⁵P. K. Kabir, *Phys. Rev. Lett.* **51**, 231 (1983).

¹⁶F. Basecq and L. Wolfenstein, Carnegie-Mellon University Report No. CMU-HEG82-12, 1983 (unpublished).

¹⁷A. Puglierin, in *Proceedings of the International Colloquium on Matter Nonconservation*, Frascati, Italy, January 1983 (to be published).

¹⁸M. L. Cherry *et al.*, *Phys. Rev. Lett.* **50**, 1354 (1983).